Quantum Electronics **46** (11) 1031–1039 (2016)

OPTICAL FIBRES DOI: 10.1070/QEL16212

Fabrication of microstructured optical fibres by drawing preforms sealed at their top end

A.N. Denisov, A.F. Kosolapov, A.K. Senatorov, P.E. Pal'tsev, S.L. Semjonov

Abstract. **This paper presents results of a theoretical analysis and a series of experiments dealing with microstructured optical fibre (MOF) drawing from preforms sealed at their top end. We demonstrate that maintaining a constant temperature in the top part of the preform is of key importance for the ability to produce long MOFs with stable parameters. We have proposed and implemented a technique for additional, controlled heating of the top part of preforms, which allows one to fabricate long MOFs with both constant and varying parameters. Evidence is provided that MOFs with holes differing in size can be produced rather easily by this method.**

Keywords: *microstructured optical fibres, photonic crystal fibres, fabrication of optical fibres.*

1. Introduction

Microstructured optical fibres (MOFs), also known as photonic crystal fibres, are becoming indispensable elements of fibre lasers owing to their unique, highly nonlinear properties. Such fibres are used for material dispersion compensation in the 1-μm range, supercontinuum generation and efficient four-wave mixing in the visible and IR spectral regions [1–6]. These effects depend significantly on the dispersion properties of the MOF, which are in turn determined by the size, position and longitudinal uniformity of the holes in the fibre. Therefore, an important issue pertaining to the MOF drawing process is the ability to maintain the structural parameters of the fibre – which are determined by those of the preform – constant or vary them in a controlled manner.

There are several main MOF drawing methods. One of them is the drawing of preforms with their holes open to the atmosphere [7–15]. In the drawing process, however, surface tension forces reduce the hole diameter, to the point of complete hole closure (collapse). To avoid hole collapse, one should use a low drawing temperature, high preform feed rate, large hole diameter or any combination of these parameters [7]. Unfortunately, drawing under such conditions leads to problems with the strength of the MOFs and the reproducibility of their parameters and makes it difficult to produce MOFs with thin walls between the holes.

One, widely used approach to preventing hole collapse during MOF drawing is to introduce a gas (typically argon, oxygen or nitrogen) into the holes at an external pressure slightly exceeding atmospheric pressure, which allows surface tension forces to be compensated for [14–21]. This method offers the possibility of working at higher temperatures and fibre drawing speeds, which ensure sufficient strength of the resultant MOFs. However, the final diameter of the holes in the fibre is then determined not only by the initial diameter of the holes in the preform but also by the temperature and drawing speed, which leads to low stability of the structural and, hence, physical parameters (e.g. dispersion) of the MOF. Moreover, if an MOF with different hole diameters is needed, different gas pressures should be used.

In this paper, we consider an alternative MOF drawing method, from preforms sealed at their top end [22, 23]. At the beginning of the process, the holes are open at the bottom end of the preform, i.e. they are at atmospheric pressure. After hole collapse in the first instance of drawing, fibre drawing and, accordingly, the decrease in preform length are accompanied by a gradual rise in internal gas pressure in the holes of the preform. Eventually, this leads to the formation of holes in the resulting MOF. However, the MOFs described by DiGiovanni et al. [22] have essentially identical relationships between the hole dimensions and spacings in both the preform and fibre, which significantly differentiates them from the MOFs produced by us using the proposed method [24, 25]. The effect of MOF length on the degree of geometric transformation of the fibre structure was not examined by DiGiovanni et al. [22]. Thus, the existing uncertainty in the geometric transformation of the MOF structure makes it impossible to control the structural parameters of MOFs fabricated by the method in question.

The objectives of this work were

(1) to perform a theoretical analysis of the MOF drawing from preforms sealed at their top end and determine the main factors influencing the transformation of the geometric structure of the MOFs in this process;

(2) to draw various MOFs from preforms sealed at their top end and compare the results with theoretical predictions;

(3) to find necessary conditions for the fabrication of long MOFs with stable structural and, accordingly, physical parameters; and

(4) to experimentally verify the possibility of controlling the parameters of MOFs through additional heating of the top part of the preform during drawing.

A.N. Denisov, A.F. Kosolapov, A.K. Senatorov, S.L. Semjonov Fiber Optics Research Center, Russian Academy of Sciences, ul. Vavilova 38, 119333 Moscow, Russia; e-mail: denisov@fo.gpi.ru;
P.E. Pal'tsev Moscow Institute of Physics and Technology (State University), Institutskii per. 9, 141707 Dolgoprudnyi, Moscow region, Russia

Received 23 September 2016; revision received 12 October 2016
Kvantovaya Elektronika **46** (11) 1031–1039 (2016)
Translated by O.M. Tsarev

2. Theoretical analysis

Consider a steady-state process. In this study, we restrict our consideration to the drawing of silica MOFs, even though there is also great interest in polymer [26] and non-silica glass [27, 28] MOFs. In examining the drawing of such MOFs, only differences in their relevant parameters should be taken into account.

Without loss of generality, consider for simplicity the drawing of a silica tube (initial outer and inner diameters D_1 and d_1) into a capillary of outer diameter D_2, with a hole of diameter d_2 (Fig. 1). Most of the conclusions drawn below are applicable as well to more general cases. Let the preform feed rate be v_1 and the capillary drawing speed be v_2. The top end of the preform is sealed. The section of the preform between the sealed end and the furnace inlet is maintained at temperature T_1 and pressure P_1. The temperature and pressure in the centre of the furnace are T_2 and P_2, respectively.

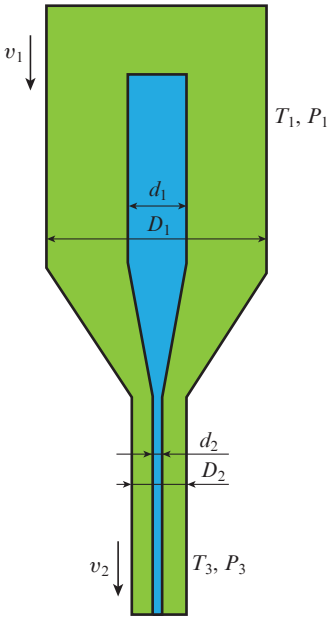

Figure 1. Schematic of capillary drawing from a preform sealed at its top end.

From the continuity condition for silica glass flow, we have

$$\frac{v_1}{v_2} = \frac{S_2}{S_1} = \frac{D_2^2 - d_2^2}{D_1^2 - d_1^2}, \tag{1}$$

where S_1 and S_2 are the cross-sectional areas of the silica glass in the preform and capillary, respectively.

It can be shown that, at typical MOF drawing parameters, the gas pressure P_1 in the holes of the preform has enough time to become constant throughout its length ($P_1 = P_2$). Consider first the simple case of a relatively small hole in a capillary, where the gas flow relative to its wall is insignificant. It follows from the gas mass balance constraint that, in a steady state,

$$\rho_1 s_1 v_1 = \rho_2 s_2 v_2, \tag{2}$$

where s_1 and s_2 are the cross-sectional areas of the air holes in the preform and capillary, respectively, and ρ_1 and ρ_2 are the gas densities in the hole in the top part of the preform and in the neck-down region, respectively. Taking into account the equation of state for an ideal gas and the fact that the gas pressure is constant throughout the length of the preform, we obtain

$$\frac{s_2}{s_1} = \frac{v_1}{v_2}\frac{T_2}{T_1}. \tag{3}$$

Taking into account (1), we have

$$\frac{s_2}{S_2} = \frac{s_1}{S_1}\frac{T_2}{T_1} = \frac{s_1}{S_1}k. \tag{4}$$

The parameter k represents the change (increase) in the relative area of the holes in the MOF with respect to that in the preform. In the case of n identical holes, (4) takes the form

$$\frac{d_2^2}{D_2^2 - nd_2^2} = \frac{d_1^2}{D_1^2 - nd_1^2}\frac{T_2}{T_1}. \tag{5}$$

In a typical case of silica glass, we have $T_1 = 300$ K and $T_2 = 2100$ K. Then, at a small number of sufficiently small holes in a preform ($\sqrt{n}\,d_1 \ll D_1$, i.e. the total area of the air holes is much smaller than the area of the preform, which corresponds to the real situation), we obtain their relative linear 'expansion' in the fibre: $(d_2/D_2)/(d_1/D_1) = \sqrt{T_2/T_1} \approx 2.65$. This differs considerably from the value reported by DiGiovanni et al. [22] ($\sim$1.05). For lack of detailed information about the MOF drawing conditions in their study [22], we can only assume that their MOFs were probably produced with the sealed ends of the capillaries located near the centre of the furnace, so that $T_2 - T_1 \sim 200$ K.

One of the most widely used structural parameters characterising MOFs is the ratio of the hole diameter (d_2) to the centre-to-centre distance between the holes (Λ_2): d_2/Λ_2. In a particular case of a small area of air holes compared to the area of silica glass ($s_1 \ll S_1$) and several (or many) identical holes spaced Λ_1 apart, taking into account that $\Lambda_1/D_1 \approx \Lambda_2/D_2$ (similarity of the geometric structure persists during fibre drawing), we can reduce (5) to the following form:

$$\frac{d_2}{\Lambda_2} = \frac{d_1}{\Lambda_1}\sqrt{\frac{T_2}{T_1}}. \tag{6}$$

At $T_1 = 300$ K and $T_2 = 2100$ K, we have $d_2/\Lambda_2 \approx (d_1/\Lambda_1)\times 2.65$. Since the hole diameter in the fibre after drawing cannot exceed the spacing between the holes, the relationship $d_2/\Lambda_2 < 1$ should be met. Then, in preform fabrication one should ensure that $d_1/\Lambda_1 < 1/2.65 \approx 0.38$. Otherwise, at $d_1 > 0.38\Lambda_1$, neighbouring holes will influence each other during the MOF drawing process and their shape will vary, but relation (4) will remain valid. The evolution of the hole shape may also be of some interest, but this problem can only be resolved using numerical mathematical modelling [29, 30], which is beyond the scope of this work.

Thus, relation (4) leads us to conclude that the expansion of the holes will be constant and stable as long as the top part of the preform (between the sealed end and the furnace inlet) will have a constant temperature, i.e. until the top end of the preform will enter the furnace.

It is worth noting that, if a preform has holes of different diameters (d_{1i}, where i refers to a group of holes of a given size), Eqn (5) takes the form

$$\frac{d_{2i}^2}{D_2^2-\sum_j n_j d_{2j}^2}=\frac{d_{1i}^2}{D_1^2-\sum_j n_j d_{1j}^2}\frac{T_2}{T_1}. \qquad (7)$$

Like (5), this relation is valid if the holes in a preform are sufficiently spaced apart, so that they do not interact during the MOF drawing process and their shape remains unchanged.

It follows from (7) that, if the total area of the air holes is much smaller than the preform area, the holes differing in size have essentially identical relative expansion values, which in general can be accurately taken into account. This allows MOFs with holes of different diameters to be fabricated rather easily (there is no need to introduce a gas at different pressures into holes of different diameters).

In the case of relatively large holes in an MOF, the above relations, including (4), should be slightly modified. One should then take into account cooling of the MOF to the temperature T_3 (near 300 K) after drawing and the corresponding reduction in gas pressure (to P_3) in the MOF, which produces a gas flux Q from the preform to the fibre through the hole of diameter d_2. The flux Q can be found using Poiseuille's equation [31]:

$$Q=\frac{\pi d_2^4}{128\eta}\frac{P_2-P_3}{L}, \qquad (8)$$

where η is the dynamic viscosity of the gas and L is the length over which the temperature of the MOF decreases to T_3. As a result, the expansion of the hole decreases slightly.

To evaluate the decrease in the case of capillary drawing, we add the mass flux of the gas, $Q\rho_2$, to the right-hand side of (2). Relation (5) then takes the following form:

$$\frac{d_2^2}{D_2^2-d_2^2}=\frac{d_1^2}{D_1^2-d_1^2}k, \qquad (9)$$

where

$$k=\frac{T_2}{T_1}\left[1+\frac{d_2^2}{32\eta L v_2}(P_2-P_3)\right]^{-1}. \qquad (10)$$

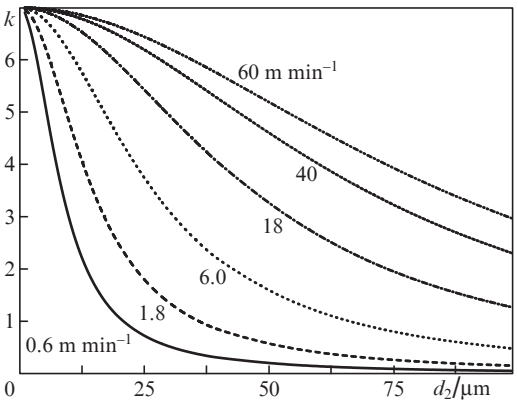

Figure 2. Parameter k as a function of hole diameter d_2 at drawing speeds in the range 0.6–60 m min^{-1}.

Thus, the expansion of sufficiently large holes in MOFs is smaller, and the decrease is determined by the hole size, MOF drawing speed, gas viscosity in the preform and the geometric parameters of the fibre-drawing tower (the length L over which the temperature of the MOF drops to T_3). Let us estimate the change in the parameter k in response to changes in hole diameter d_2 from 1 to 100 μm and in drawing speed v_2 from 0.6 to 60 m min^{-1} at a length $L = 0.25$ m, pressure difference $P_2 - P_3 = 1.02$ atm and argon viscosity $\eta = 8.97 \times 10^{-4}$ P (2100 K) [32] (Fig. 2). It is seen in Fig. 2 that, at $d_2 = 50$ μm and $v_2 = 18$ m min^{-1} (near that typical of silica MOFs), the parameter k decreases by about a factor of 2 compared to its initial level.

3. Experimental results

To verify theoretical calculation results, we fabricated several MOFs from different preforms.

3.1. Capillary drawing

A capillary was drawn from a silica tube of diameter $D_1 = 6.2$ mm with a hole diameter $d_1 = 4.4$ mm. The drawing speed was $v_2 = 40$ m min^{-1} and the preform feed rate was $v_1 = 10^{-2}$ m min^{-1}. During drawing, we monitored the outer diameter of the capillary, D_2. After that, we determined its inner diameter d_2 using relation (1) and then the parameter k using (9). Figure 3a shows the variation in k as the preform is lowered to the furnace. The position of the sealed end of the pre-

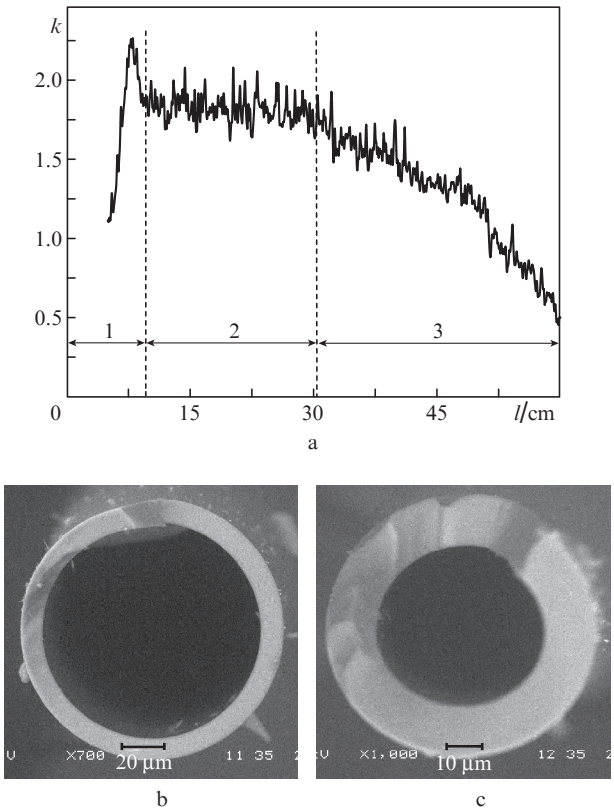

Figure 3. (a) Parameter k as a function of the position l of the sealed end of the preform during capillary drawing; (b, c) cross-sectional electron micrographs of the capillary in regions 2 (l = 14 cm) and 3 (l = 59 cm), respectively.

form, l, was measured from that in the first instance of drawing. The first region of the variation in l (region 1) corresponds to the settling of hole expansion in the capillary. At the beginning of drawing, heating the preform to a temperature T_2 leads to hole collapse under the effect of surface tension forces. During subsequent drawing, however, the length of the preform and, accordingly, the gas volume in the hole decrease, raising the pressure in the hole. This continues until the pressure surpasses the surface tension, leading to the formation of a hole. The hole is initially very small, so the decrease in gas volume in the preform is insignificant, the pressure in the hole continues to rise, and the hole in the capillary grows. The process continues until the system reaches equilibrium, as represented by (2).

Next, a steady state sets in (region 2), in which the gas pressure in the hole, capillary diameter D_2 and hole diameter d_2 remain constant and, hence, the parameter k is also stable. In this region, we have $D_2 = 122$ μm and $d_2 = 99$ μm (Fig. 3b), which makes it possible to find k using (10): ~2 (Fig. 2). Thus, the measured k agrees rather well with the calculated one, and in this case it is important to take into account the rather large capillary size d_2.

The capillary geometry remains unchanged as long as the temperature T_1 of the top part of the preform remains constant. At the same time, when the sealed end approaches the furnace and crosses its upper edge ($l = 30$ cm), the temperature T_1 begins to rise sharply (region 3). According to (10), this causes a corresponding decrease in k. Figure 3c shows a micrograph of the resultant capillary at $l = 59$ cm.

3.2. Drawing of a six-hole MOF

A preform was made by drilling holes in a silica monolith. Next, it was stretched to reduce its diameter and jacketed in a silica tube to increase the MOF length at a desired core size. The drawing speed v_2 was about 20 m min^{-1}. Its exact value was set by a servo system, which monitored the outer diameter of the MOF ($D_2 = 125$ μm). The drawing temperature was $T_2 = 2113$ K. Figures 4a–4d show cross-sectional electron-microscopic images of the MOF at a constant magnification and different positions of the sealed end of the preform (l). Figure 4e shows a cross-sectional optical photograph of the preform.

Since the preform had relatively large holes ($d_1 \approx 0.7\Lambda_1$), their shape began to change when expansion exceeded some threshold (Figs 4c, 4d). Note also that, in the cross section of the MOF in Fig. 4a, the d_2/Λ_2 ratio is much less than d_1/Λ_1. Therefore, this image of the MOF corresponds to the instant of hole formation as a result of the increase in gas pressure, which surpasses the surface tension.

Figure 5 shows the measured outer diameter of the six-hole structure (D_{str}), core diameter (D_{core}) and k as functions of the position of the sealed preform end. As in the case of capillary drawing, the variation in l can be tentatively divided into three steps. The first step is the settling of hole expansion in the MOF. Note that a region about 6 cm in length has no holes because of the hole collapse in the first instance of drawing. Next, at $l = 16$ cm, a steady expansion state sets in, in which the pressure and hole diameter should not vary further. This is, however, not quite so for the MOF under consideration: the hole expansion in the fibre gradually decreases, which seems to result from the heating of the preform by the IR radiation from the furnace, because silica glass prevails in the cross section of the preform. Heating of

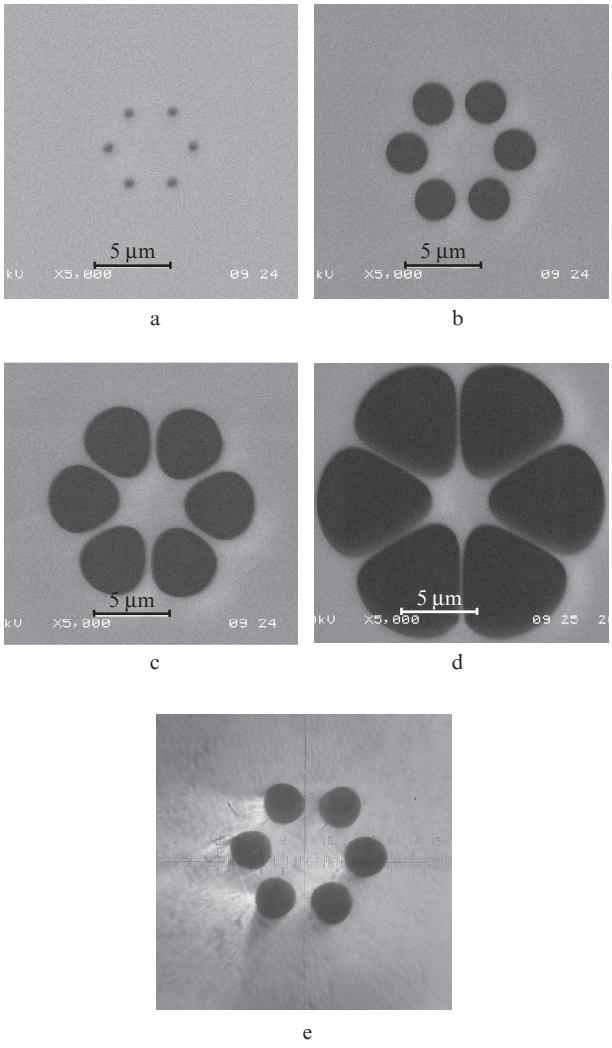

Figure 4. Cross-sectional micrographs of a six-hole MOF at l = (a) 6, (b) 12, (c) 14 and (d) 16 cm and (e) cross-sectional optical photograph of the preform.

the preform is nonuniform, with a certain temperature gradient, which shows up as a gradual variation in hole expansion until $l \sim 40$ cm is reached. Finally, as the length of the

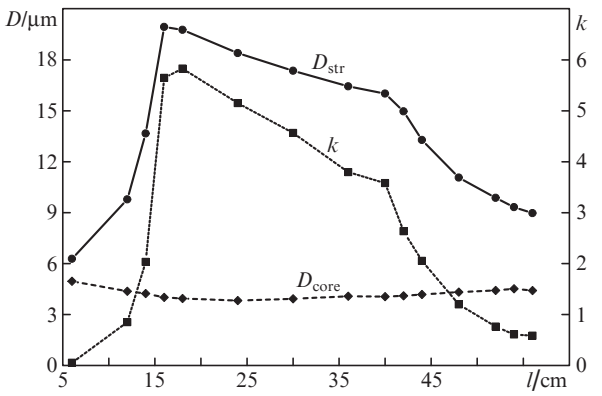

Figure 5. Measured outer diameter of a six-hole structure (D_{str}), core diameter (D_{core}) and k as functions of the position of the sealed preform end, l.

preform decreases during the MOF drawing process, its sealed end crosses the upper edge of the furnace (this instant corresponds to a distance $l = 40$ cm) and the temperature T_1 begins to rise more rapidly. This leads to a sharp decrease in hole expansion, in accordance with (4), as clearly seen in Fig. 5.

3.3. MOF drawing with an additional heater for the top part of the preform

The present experimental data demonstrates that the main cause of the instability of the parameters of the MOFs is the nonuniform heating of the top part of the preform, which leads to variations in hole expansion during the drawing process. To produce long MOFs with constant geometric and physical parameters, the temperature of the top part of the preform should be maintained constant. A relatively simple approach is to use a specially designed additional heater for the top part of the preform (it is more difficult to cool the preform and stabilise its temperature). The heater should ensure a controlled longitudinal temperature profile to compensate for variations in the temperature of the top part of the preform. The degree of hole expansion in the MOFs is determined by the variation in average temperature. Moreover, setting a predetermined temperature profile with such a heater, one can fabricate MOFs with a constant outer diameter and varied hole diameter, i.e. with longitudinal variations in optical parameters.

Figure 6 shows a schematic of MOF drawing with an additional heater for controlling the temperature of the top part of the preform. The top end of the preform (*1*) is sealed and fused to an auxiliary rod (*2*), secured to the preform feed system. The feed system ensures a necessary rate of preform feed to the furnace (v_1). The furnace (*3*) heats the preform to the drawing temperature. The temperature in the centre of the furnace – in the neck-down region for silica glass – is $T_2 \approx 2143$ K. The MOF (*4*) is drawn from the bottom end of the preform with the use of a take-up capstan, which ensures the desired rate of the process, v_2. The top part of the preform is enclosed in the additional heater (*5*) and is maintained at temperature T_1, which can be varied from room temperature to ~1200 K. Between the heater and furnace is a flange (*6*) for mounting diaphragms.

A key component of the heater is a 42-cm-long ceramic tube (outer diameter, 23 mm; inner diameter, 18 mm), with three independent Nichrome tape sections, each 13 cm in length, wound on it. The electric power supplied to them can be varied in a wide range or switched off.

Figure 7a shows the measured heater temperature as a function of the position of the thermocouple (l) as measured from the upper edge of the heater towards the drawing furnace. Negative l values correspond to positions above the heater. Curve I was obtained with the heater switched off and the drawing furnace switched on. The temperature in the furnace was $T_2 = 1973$ K. Curve II corresponds to the drawing furnace switched off, with the heater ensuring a negative temperature gradient in the direction of the furnace in order to compensate for the heating of the preform under its effect. Curve III was obtained with the middle section of the heater switched off, which ensured the maximum possible temperature gradient in it.

Figure 7b presents $k(l)$ curves obtained from the above experimental data. In our calculations, we assumed that, when moving, the preform was heated and cooled instantaneously, so that the relation $k = T_2/T_1(l)$, valid for small holes in MOFs, was applicable.

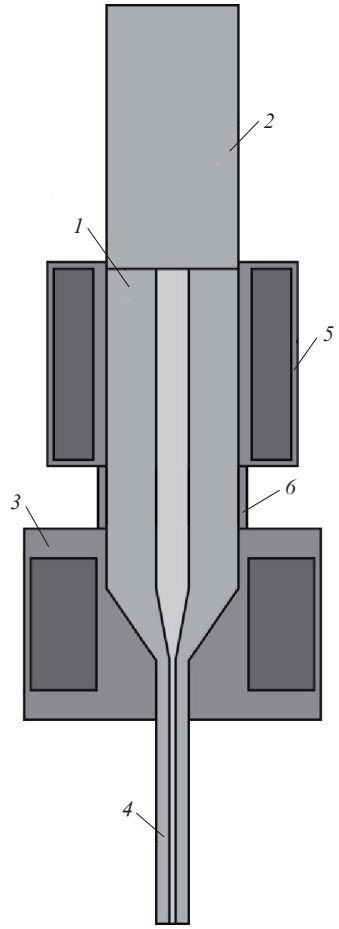

Figure 6. Schematic of MOF drawing with an additional heater of the top part of the preform.

The shape of curve I indicates that, as the preform approaches the furnace, the temperature along it rises by more than 150 K. Extrapolating this curve to $l = 67$ cm (which corresponds to the upper edge of the drawing furnace), we obtain an increase in temperature by more than 300 K. According to (4), such a change in temperature should be accompanied by a decrease in the degree of hole expansion to $k \sim 3.5$, in good agreement with the experimental data presented in Fig. 5.

To demonstrate the potentialities of MOF drawing with an additional heater, we used a highly birefringent microstructured fibre (HB MSF) with a *724* structure [33, 34] (two rings of holes). The HB MSF preform was made by drilling holes in a silica monolith. The hole diameter was 2.1 mm in one ring and 2.5 mm in the other. The spacing between the holes in the former ring was $\Lambda_1 = 3.4$ mm, with $d_{1\text{in}}/\Lambda_1 = 0.62$. This was expected to ensure $d_{2\text{in}}/\Lambda_2 = 0.92 < 1$ [see (6)] after preform drawing at an additional heater temperature of 973 K. The preform was then stretched to a smaller diameter and jacketed in a silica tube to increase the fibre length and ensure the desired core size.

This structure is of interest from the viewpoint of a detailed experimental study of MOF drawing from multihole preforms sealed at their top end, in which holes having

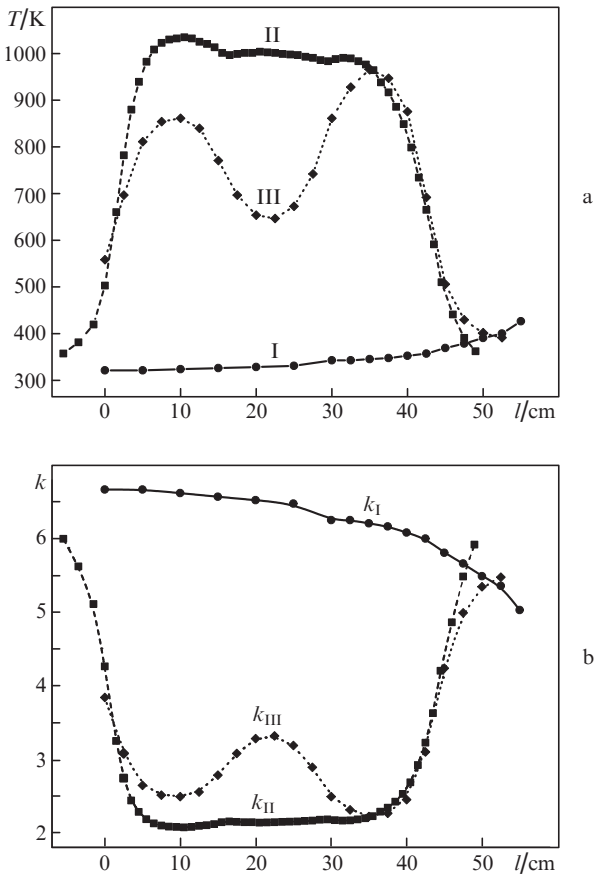

Figure 7. (a) Measured heater temperature as a function of the position of the thermocouple relative to the upper edge of the heater (I) without heating and with (II) three and (III) two windings energised; (b) parameter k as a function of the position of the sealed end of the preform (calculation from the above data).

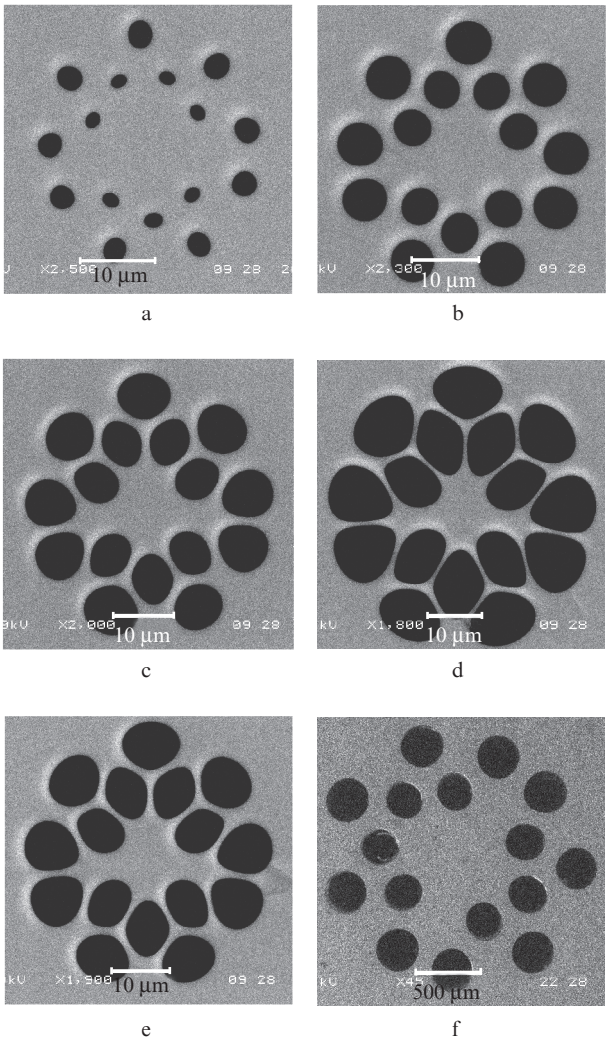

Figure 8. Cross-sectional micrographs of HB MSF *724* produced by drawing at a constant heater temperature profile: position of the sealed end of the preform l = (a) –10.8, (b) –8.7, (c) –5.1, (d) +0.2 and (e) +17.9 cm; (f) micrograph of the cane for drawing HB MSF *724*.

different sizes and neighbours are located at different distances from the centre of the preform. For further analysis, we tentatively divided such holes into four groups. The k values for these groups of holes are denoted as $k1$, $k2$, $k3$ and $k4$.

3.3.1. MOF drawing at a constant heater temperature profile. During drawing, the heater operation mode corresponded to curve II (Fig. 7a). In the initial position (before the beginning of drawing), the sealed end was 13 cm above the upper edge of the heater (i.e. $l = -13$ cm). The preform feed rate during drawing was $v_1 = 10^{-2}$ m min^{-1} and the drawing speed was $v_2 \approx 30$ m min^{-1}. The exact value of the latter was determined by a servo system, which ensured an outer diameter of the MOF $D_2 = 125$ μm. The drawing temperature was $T_2 = 2113$ K. Figures 8a–8e show cross-sectional electron-microscopic images of HB MSF *724* at different values of l and Fig. 8f shows a cross-sectional image of the cane.

Figure 9 shows the measured parameters k and $k1$–$k4$ as functions of the position of the sealed end of the preform, l, and a $k_{II}(l)$ curve calculated from a previously measured temperature profile. Note first of all the relatively small variations of the measured parameters $k1$–$k4$ from the corresponding k values. Thus, we are led to conclude that, in this MOF configuration, the expansion parameters of the holes, which differ in size and neighbours, almost coincide, in accor-

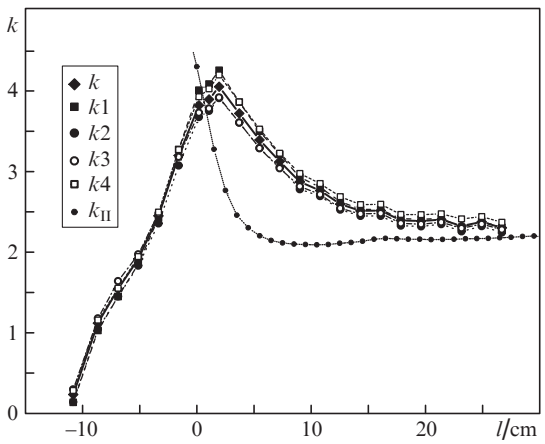

Figure 9. Measured parameters k and $k1$–$k4$ as functions of the position of the sealed end of the preform, l, during drawing at a constant heater temperature profile and $k_{II}(l)$ evaluated from a measured temperature profile.

dance with relation (7), which was used to analyse MOFs with round holes. Note that, in this case, because of the small hole size in the MOF, with the possible gas flow in the holes taken into account [see (10)], the difference in k between the holes of different diameters is within 2%.

In a steady state (at $l > +18$ cm), the measured values of k differ from the calculation results by no more than 10%. This attests to good accuracy of the proposed analytical model for the transformation of the geometric structure of MOFs during drawing from preforms sealed at their top end.

The process of reaching a steady-state value of the expansion parameter k has several characteristic features. At the beginning of drawing, the expansion of the holes in the outer ring exceeds that in the inner ring (Fig. 8a), which may be caused by the radial temperature gradient in the neck-down portion of the preform. This process can be broken down into two steps (Fig. 9). The first step is a relatively slow rise in k to a value corresponding to the calculated k_{II} (at $l = +0.2$ cm). Next, since the heater temperature rises after this position of the sealed end of the preform and, accordingly, k_{II} drops to a predetermined constant level, the parameter k begins to decrease. The decrease is relatively slow, roughly exponential:

$$k = k_0 + \Delta k \exp(-t/\tau), \tag{11}$$

where $k_0 = 2.26$; $\Delta k = 2.45$; and $\tau = 6.75$ min (with allowance for the rate $v_1 = 10^{-2}$ m min^{-1}). This manner of reaching a steady-state value of the parameter k (in both regions) is probably due to the rather low drawing temperature ($T_2 = 2113$ K, which roughly coincides with the lower boundary of the working drawing temperature for silica glass) and, hence, to the relatively high viscosity of silica, which is an exponential function of temperature [30]:

$$\mu = 5.8 \times 10^{-7} \exp\left(\frac{515400}{RT}\right), \tag{12}$$

where $R = 8.31446$ J mol^{-1} K^{-1} is the gas constant.

The untimely termination of drawing (at $l = +26.7$ cm) is caused by MOF breakage, probably because of small damage to the preform when it was lifted to the drawing tower. Subsequently, this problem was eliminated using an additional means to protect the preform from touching the metallic elements of the drawing tower during uplift.

3.3.2. MOF drawing at a varied heater temperature profile. During drawing, the heater operation mode corresponded to curve III (Fig. 7a). In the initial position (before the beginning of drawing), the sealed end of the preform was 9 cm above the upper edge of the heater ($l = -9$ cm). The preform feed rate during drawing was $v_1 = 1.45 \times 10^{-2}$ m min^{-1} and the drawing speed was $v_2 \approx 38$ m min^{-1}. The outer diameter of the MOF was $D_2 = 125$ μm and the drawing temperature was $T_2 = 2163$ K. Figure 10 shows cross-sectional electron-microscopic images of HB MSF *724* at a constant magnification and different values of l.

Figure 11 shows the measured parameters k and $k1-k4$ as functions of l, and k_{III} calculated from a previously measured temperature profile. As in the case of the previous experiment, it is worth noting the relatively small variations of the measured parameters $k1-k4$ from k. Note that here we deal precisely with a quasi-steady state, because the temperature

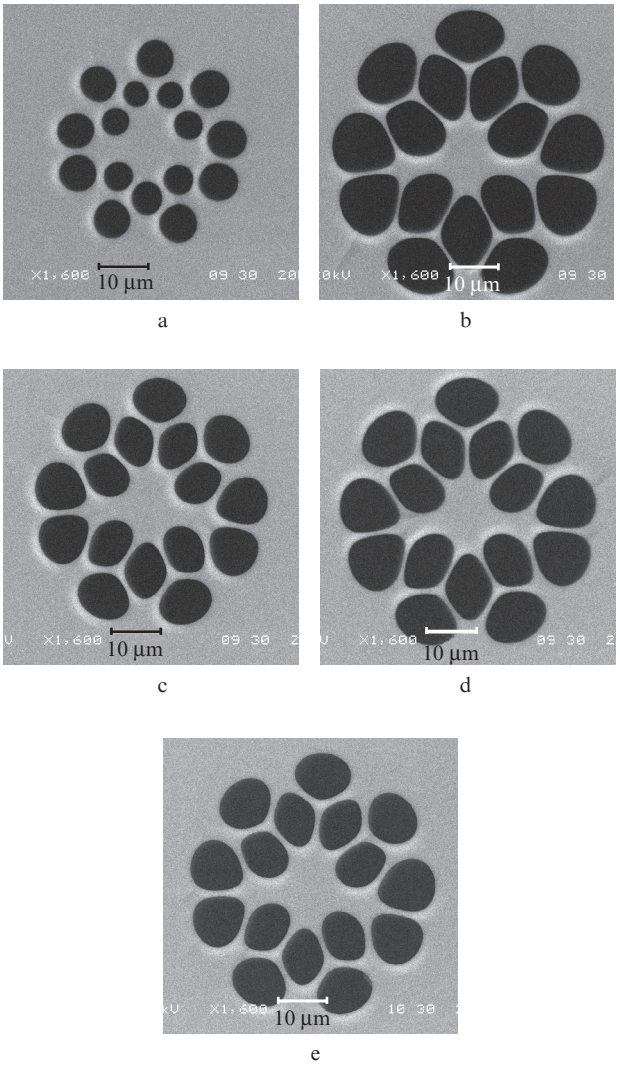

Figure 10. Cross-sectional micrographs of HB MSF *724* during drawing at a varied heater temperature profile: position of the sealed end of the preform l = (a) –7.0, (b) –3.0, (c) +4.9, (d) +24.6 and (e) +40.3 cm.

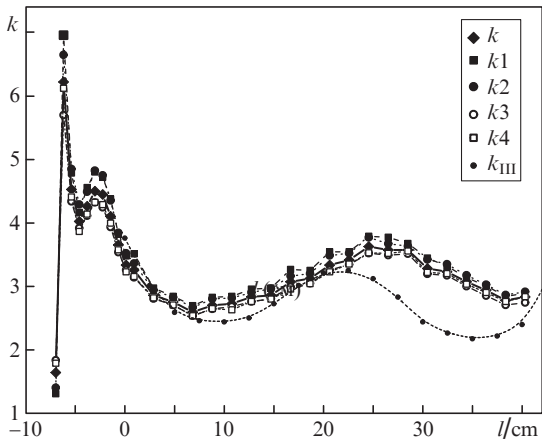

Figure 11. Measured parameters k and $k1-k4$ as functions of the position of the sealed end of the preform, l, during drawing at a varied heater temperature profile and k_{III} evaluated from the measured temperature profile.

profile along the heater is varied and, as a result, the parameter k also varies during the MOF drawing process. Nevertheless, under these drawing conditions, too, in the MOF configuration in question the expansion parameters of different holes (which differ in size and neighbours) almost coincide.

The results obtained in a quasi-steady state (l = +3.0 to +38.4 cm) differ somewhat from those described above. Note first of all the excellent agreement between the experimentally determined values of the parameter k and the calculated k_{III} immediately after a quasi-steady state is reached (l = +3.0 cm), which attests to good accuracy of the proposed analytical model. Next, as would be expected, there is a discrepancy between the measured k and k_{III} obtained under the assumption that, when moving, the preform was heated and cooled instantaneously. Actually, there are nonzero heating and cooling times, which differ from each other. Because of this, when a preform moves in a varying temperature field, the gas pressure in the holes and, as a consequence, the parameter k exhibit complex behaviour, which can only be assessed by numerical techniques, but this lies beyond the framework of this work. At the same time, it is seen from Fig. 11 that the magnitude and range of the parameter k agree rather well with calculation results, which demonstrates practical feasibility of fabricating long MOFs with parameters varying along their length.

In this experiment, a quasi-steady-state value of the parameter k is reached much more rapidly than in the preceding case and has a number of local maxima, at l = –6.2, –3.0 and +0.9 cm, which reflect the damped oscillatory character of the process. Thus, the entire process occurs as the preform travels just ~8 cm, which is considerably smaller than in the preceding case (about 29 cm). This can be accounted for by the higher drawing temperature T_2 and, hence, the lower viscosity of the silica glass. As in the above experiment, holes in the MOF were formed at the very beginning of the drawing process, at l = –7.0 cm (Fig. 10a), but the parameters k_i were much greater (Fig. 11) and differed less.

Comparison of the two experiments in which an MOF was drawn using an additional heater for the top part of the preform (Figs 9, 11) indicates that the time needed to reach a steady or quasi-steady state depends significantly on the temperature in the drawing furnace, T_2, which determines the viscosity of the silica glass in the neck-down region. According to (12), the viscosity of silica glass varies by about a factor of 2 across the working range of MOF drawing temperatures (2113–2163 K). Thus, comparison of the variations in k in the two experiments suggests that the optimal drawing temperature is near 2163 K or slightly lower.

It is seen in Fig. 11 that, for the heater used in this study, the working range of preform displacements is about 31 cm. A similar range can be ensured at a constant heater temperature profile if the drawing temperature exceeds that in our first experiment. This range of preform displacements corresponds to an about 800-m length of the MOF in this study at an outer preform diameter of ~6 mm. A simple calculation shows that a preform with a standard diameter of 8 mm can be drawn into an MOF more than 1200 m in length and 125 μm in diameter.

4. Conclusions

MOF drawing from preforms sealed at their top end has been analysed using numerical techniques, and a simple analytical model has been proposed that describes the transformation of the geometric structure of the MOF in this process. Experimental data for various MOFs drawn from preforms sealed at their top end agree well with theoretical estimates, demonstrating that maintaining a stable temperature in the top part of the preform is of key importance for the ability to produce long MOFs with constant parameters. It has also been shown that, in the case of sufficiently large holes in MOFs, one should take into account additional corrections to the transformation of the geometric structure during fibre drawing.

It has been demonstrated experimentally that additional, controlled heating of the top part of preforms makes it possible to fabricate long MOFs (more than 1200 m in length) with both constant and varying parameters. Experimental evidence has been provided that MOFs with holes differing in size can be produced rather easily by this method.

Acknowledgements. We are grateful to E.M. Dianov for his continuous interest in and support of this work.

This work was supported by the Russian Foundation for Basic Research (Grant No. 15-02-996788 A).

References

1. Ferrando A., Silvestre E., Andres P., Miret J., Andres M. *Opt. Express*, **9**, 687 (2001).
2. Saitoh K., Koshiba M., Hasegawa T., Sasaoka E. *Opt. Express*, **11**, 843 (2003).
3. Hartung A., Heidt A.M., Bartelt H. *Opt. Express*, **19**, 7742 (2011).
4. Zhang W.Q., Ebendorff-Heidepriem H., Monro T.M., Afshar V.S. *Opt. Express*, **19**, 21135 (2011).
5. Herzog A., Shamir A., Ishaaya A.A. *Opt. Lett*., **37**, 82 (2012).
6. Sylvestre T., Ragueh A.R., Lee M.W., Stiller B., Fanjoux G., Barviau B., Mussot A., Kudlinski A. *Opt. Lett*., **37**, 130 (2012).
7. Fitt A.D., Furusawa K., Monro T.M., Please C.P. *J. Lightwave Technol*., **19**, 1924 (2001).
8. Fitt A.D., Furusawa K., Monro T.M., Please C.P., Richardson D.J. *J. Eng. Math*., **43**, 201 (2002).
9. Xue S.C., Tanner R.I., Barton G.W., Lwin R., Large M.C.J., Poladian L. *J. Lightwave Technol*., **23**, 2245 (2005).
10. Xue S.C., Tanner R.I., Barton G.W., Lwin R., Large M.C.J., Poladian L. *J. Lightwave Technol*., **23**, 2255 (2005).
11. Xue S.C., Large M.C.J., Barton G.W., Tanner R.I., Poladian L., Lwin R. *J. Lightwave Technol*., **24**, 853 (2006).
12. Voyce C.J., Fitt A.D., Monro T.M. *J. Lightwave Technol*., **26**, 791 (2008).
13. Stokes Y.M., Buchak P., Crowdy D.G., Ebendorff-Heidepriem H. *J. Fluid Mech*., **755**, 176 (2014).
14. Luzi G., Epple P., Scharrer M., Fujimoto K., Rauh C., Delgado A. *J. Lightwave Technol*., **28**, 1882 (2010).
15. Chen M.J., Stokes Y.M., Buchak P., Crowdy D.G., Foo H.T.C., Dowler A., Ebendorff-Heidepriem H. *Opt. Mater. Express*, **6**, 166 (2016).
16. Russell P.St.J., Birks T.A., Knight J.C. U.S. Patent 6888992B2 (2005).
17. Wynne R.M. *J. Lightwave Technol*., **24**, 4304 (2006).
18. Boyd K., Ebendorff-Heidepriem H., Monro T.M., Munch J. *Opt. Mater. Express*, **2**, 1101 (2012).
19. Chen Y., Birks T.A. *Opt. Mater. Express*, **3**, 346 (2013).
20. Kostecki R., Ebendorff-Heidepriem H., Warren-Smith S.C., Monro T.M. *Opt. Mater. Express*, **4**, 29 (2014).
21. Chen M.J., Stokes Y.M., Buchak P., Crowdy D.G., Ebendorff-Heidepriem H. *J. Fluid Mech*., **783**, 137 (2015).
22. DiGiovanni D.J., Vengsarkar A.M., Wagener J.L., Windeler R.S. U.S. Patent 5802236 (1998).
23. Voyce C.J., Fitt A.D., Hayes J.R., Monro T.M. *J. Lightwave Technol*., **27**, 871 (2009).
24. Semjonov S.L., Denisov A.N., Dianov E.M., in *Specialty Optical Fibers, OSA Techn. Digest* (Opt. Soc. Am., 2012) STu1D.4.

25. Semjonov S.L., Denisov A.N., Senatorov A.K. *Proc. SPIE Int. Soc. Opt. Eng*., **8961**, 896129 (2014).
26. Argyros A. *J. Lightwave Technol*., **27**, 1571 (2009).
27. Liao M., Yan X., Duan Z., Suzuki T., Ohishi Y. *J. Lightwave Technol*., **29**, 1018 (2011).
28. Liao M., Gao W., Duan Z., Yan X., Suzuki T., Ohishi Y. *Opt. Express*, **20**, 1141 (2012).
29. Luzi G., Epple P., Scharrer M., Fujimoto K., Rauh C., Delgado A. *J. Lightwave Technol*., **30**, 1306 (2012).
30. Jasion G.T., Shrimpton J.S., Chen Y., Bradley T., Richardson D.J., Poletti F. *Opt. Express*, **23**, 312 (2015).
31. Sutera S.P., Skalak R. *Ann. Rev. Fluid Mech*., **25**, 1 (1993).
32. Dawe R.A., Smith E.B. *J. Chem. Phys*., **52**, 693 (1970).
33. Denisov A.N., Levchenko A.E., Semjonov S.L., Dianov E.M. *Kvantovaya Elektron*., **41**, 243 (2011) [*Quantum Electron*., **41**, 243 (2011)].
34. Denisov A.N., Semjonov S.L., Astapovich M.S., Senatorov A.K. *J. Lightwave Technol*., **33**, 5184 (2015).